Calculations on Sediment Particle Trajectory Placed in Swash Zone

Md. Azharul Hoque Student Dept. of Ocean Civil Engineering, Kagoshima University
Toshiyuki Asano Member Dept. of Ocean Civil Engineering, Kagoshima University

1. Introduction

Nearshore processes such as hydrodynamics of the waves and current and the associated mechanics of sediment transport are very complex phenomena in coastal zone. Calculation of sediment transport still relies heavily on empirical and semi-empirical relations, although progress has been made in the hydrodynamic modeling. The hydrodynamics in the swash zone is dominated by the interaction of the run up of waves with the backwash of the preceding waves, which can be an important phenomena for total sediment transport in this region. Asano (1996) reported the non-vanishing zigzag sediment movement even for the land ward region of the still water shoreline.

The present work is the first result of a continuing research to develop a computational model of two-dimensional sediment transport in the swash zone. A time dependent computational model for tracing a bed load particle has been developed. Hydrodynamic modeling has been performed based on the Carrier and Greenspan (1958)'s analytical solution for the shallow water motion of temporally periodic, finite-amplitude, non-breaking standing waves on a beach of constant slope.

2. Numerical Analysis

(a) Swash zone hydrodynamics

The *x*- axis is taken positive to the offshore direction with *x*=0 at the still water shoreline (SWSL). The beach is considered to be of uniform slope, s, having contours straight and parallel to the shoreline. The non-linear shallow water equations for cross-shore propagation are:

$$(\eta+h)_t+[u(\eta+h)]_x=0 \qquad (1)$$

$$u_t+uu_x+g(\eta+h)_x=gh_x \qquad (2)$$

where, *h*: is the undisturbed water depth, η: water surface elevation from SWL and *u*: depth averaged water particle velocities.

To solve the above nonlinear equation set, Carrier and Greenspan (1958) proceeded to consider the independent variables *x*, *t* as functions of the Rieman's invariants of the hyperbolic system and, after some afford, they were able · deduce a nonlinear and implicit change of variables which transformed the set of two nonlinear equations into a single linear equation as:

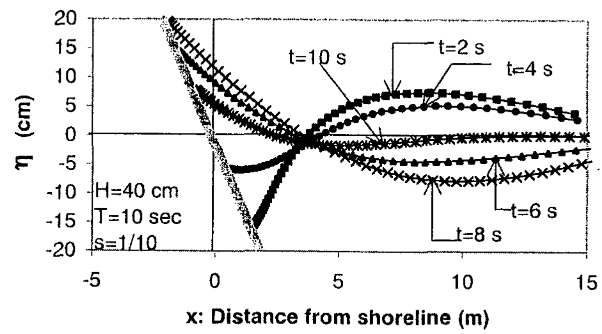

Figure 1: Temporal variation of water surface elevation

$$(\sigma\psi_\sigma)_\sigma=\sigma\psi_{\lambda\lambda} \qquad (3)$$

The new variables σ and λ are space and time-like coordinates respectively holding the relationship $(x,\ t)\approx(\sigma^2/16,\ \lambda/2)$. In the $(\sigma,\ \lambda)$ space, the instantaneous shoreline is at $\sigma=0$. The equivalent equations to eqs. (1) and (2) in terms of variables (σ,λ) are given by:

$$u=-m\frac{\psi_\sigma}{\sigma};\quad x=\frac{u^2}{2m}+\frac{\sigma^2}{16m}+\frac{\psi_\lambda}{4};\quad t=\frac{1}{m}\left(u-\frac{\lambda}{2}\right);\ \eta=-s\left(x-\frac{\sigma^2}{16m}\right)=-s\left(\frac{u^2}{2m}+\frac{\psi_\lambda}{4}\right) \qquad (4)$$

The temporal variations of water surface elevation obtained from the above solution for *H*=40 cm *T*=10 sec is shown in Fig. 1.

(b) Particle trajectory in swash zone

Instantaneous behavior of a single spherical particle placed on a uniform slope is simulated under swash motion obtained from the above formulation using the momentum equation for the particle given by:

$$\rho\frac{\pi}{6}d^3S\frac{\partial u_s}{\partial t}=\frac{1}{2}\varepsilon C_D\rho\frac{\pi}{4}d^2|u-u_s|(u-u_s)+\varepsilon(1+C_A)\rho\frac{\pi}{6}d^3\frac{\partial u}{\partial t}-\rho\frac{\pi}{6}d^3Sg\sin\theta-\left(\rho\frac{\pi}{6}d^3Sg\cos\theta-\varepsilon C_L\frac{\pi}{4}d^2(u-u_s)^2\right)\tan\phi \qquad (5)$$

in which, C_D, C_A and C_L: drag, added mass and lift force coefficient; g : gravitational acceleration, ρ:density of fluid; *d*: particle diameter; *S*: specific gravity of sediment grain; θ: beach slope angle; ϕ: internal friction angel of bed material; ε: sheltering coefficient *u*, u_s: fluid and sediment particle velocity respectively. In the present calculation C_D= 2.0; C_A=1.0, C_L=0.1C_D, ϕ=45[0] and ε= 0.4 are used.

The instantaneous fluid velocity has been obtained for all calculation grids, and the fluid velocity at the exact position of the sediment particle has been computed by interpolation. Calculations have been performed for the duration of one wave period using time increment Δt=T/1000 with initial time, t=0, at the maximum rundown. Sediment velocity has been calculated by corrector-predictor method. The instantaneous position of the particle is calculated by integrating sediment particle velocity, u_s, with a time increment. If the initial position of the sediment particle is in the dry region, smoothing average of the fluid velocity has been considered to avoid sudden change of the velocity profile. The tracing calculations are started with an initial position of sediment particle, S_{x0}, determined as a distance from the SWSL.

3. Computational Results:

Figure 2 illustrates the instantaneous shoreline position X_{shore}, sediment position S_x, fluid velocity u corresponding to the sediment position and sediment velocity u_s during one wave period for the initial position at 20 cm onshoreward from SWSL. It can be seen that the particle moves to onshore direction until the shoreline reaches to the point of maximum run-up, after which it starts to move to the offshore direction and the net displacement is found to be slightly offshore directed.

Figure 3 illustrates the net displacement of particles for different sediment sizes d. Substantial offshore-directed displacement can be observed for the particles situated in the swash region where the bed is immersed and dried alternately corresponding to run-up and run-down motion. Though the displacement pattern is uniform in the offshore region, there are some sharp changes of the displacement patterns in the swash zone having maximum displacement for the initial position in some offshore locations near the still water shoreline. In the offshore region displacement of larger particles is higher than that of smaller particles, whereas in the swash zone smaller particle also shows more displacements at some locations.

Figure 4 shows the net displacements pattern of a particle for different slope steepness, s. The milder the bottom slope the longer the swash region with more fluctuations of the displacement pattern. The displacement of the sediment particle is greater in case of steeper beach slope. The net displacements of a particle for different wave heights are shown in figure 4. The higher the wave height, the longer the swash region and higher the net displacement of the particle.

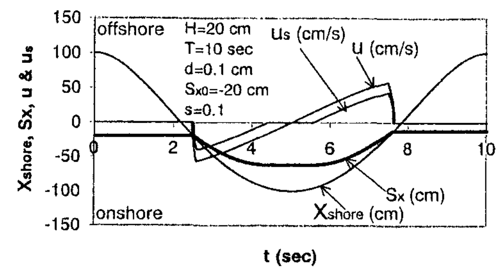

Fig. 2: Temporal variation of shoreline position X_{shore}, particle position S_x, fluid velocity u, and particle velocity u_s

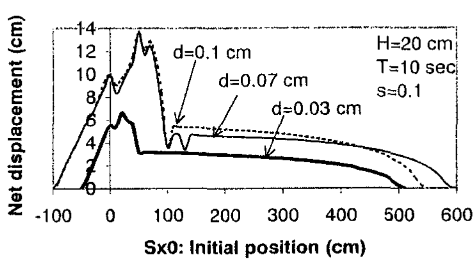

Figure 3: Net displacement during one wave period for different grain size and initial position

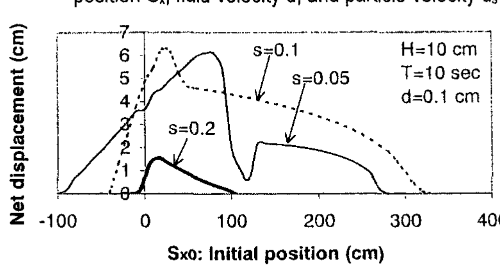

Figure 4: Net displacement during one wave period for different beach slope and initial position

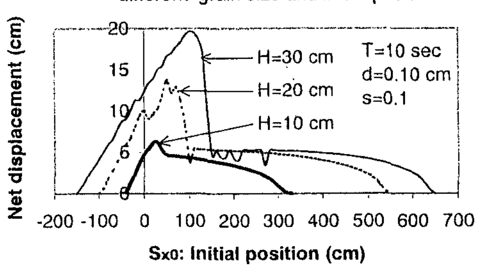

Figure 5: Net displacement during one wave period for different wave height and initial position

4. Conclusions:

Present model enables to predict the cross-shore trajectory of bed load particles in swash zone. There is a net seaward displacement of sediment particle having maximum displacement at seaward locations near the still water shoreline.

References:

1. Asano, T. (1996): Sediment transport in swash zone under obliquely incident waves, Proc. of 26th I.C.C.E, ASCE, pp.3770-3784.
2. Carrier, G. F. & Greenspan, H. P. (1958): Water waves of finite amplitude on a sloping beach, J. Fluid Mech, 4, 97-109.
3. Kobayashi, N. (1982): Sediment Transport on a gentle slope due to waves, J. Waterways, Port, Coastal and Ocean Div., Vol. 108, No. WW3, pp. 254-271.